

THE BEAM INSTRUMENTATION OF SSRF

K.R.Ye W.M.Zhou Y.Z. Chen Y.Yang R.X.Yuan S.H Tang Z.P.Liu W.Xiong Y. Sun

Shanghai National Synchrotron Radiation Center, P.O.Box 800-204, Shanghai 201800, P.R.China

Abstract

The SSRF beam diagnostic system preliminary engineering design and two of preliminary items have been completed in the beginning of this year. They are the beam position monitor and test bench; visible light data acquiring and processing research. This paper describes the beam instrumentation system of SSRF. These diagnostics must offer precise and sufficient information on the beam and machine so that the accelerator physicists and machine operators can improve the injection efficiency, optimize the lattice parameters, monitor the beam behavior. In this paper, the preliminary design of beam diagnostic and test results of prototype will be described.

1 INTRODUCTION

The SSRF is the third synchrotron radiation facility which is designed to produce high brightness and high flux X-ray in the photon energy region of 0.1~40 keV. It will be constructed in a new scientific research facility in Shanghai. The SSRF complex consists of a 300MeV linear accelerator, a 3.5 GeV booster synchrotron, and a 3.5 GeV storage ring. RF frequency is 499.65MHz.

The SSRF R&D hardware items have been completed. Acceptance test of all the items is finished in this March. Currently, testing is carried out on the following items: beam position monitor and test bunch and synchrotron radiation measurement for beam diagnostic. Machine parameters of SSRF is list in Table 1

Table 1. The main parameters of SSRF

Parameter	Storage Ring	Booster
RF Freq.(MHz)	499.65	499.65
Natural Emitance(nm-rad)	≈ 10	
Harmonic No.	660	264
Rev. Period (μ s)	1.32	0.528
Charge for single bunch(nC)	6.6	4.83
Charge for multi-bunch(nC)	0.66	
Signal bunch current(mA)	5	0.91
Mutil-bunch current(mA)	200-300	
Bunch length (2σ) (PS)	30.6 (σ =4.59mm)	
Tunes Qx, Qy	22.19/8.32	7.21/4.18
Repetition Freq.(Hz)		1

Instrumentation, which is used for the measurement of the basic accelerator parameters in the initial phases of commissioning, as well as during regular operation, plays a central role in the accelerator. We focus on a few instruments which are usable in both modes and which will allow the determination of most of the basic accelerator parameters.

There are different type monitors will be used for storage ring, Booster and Linac. Table 2 lists the monitors and subsystems that will be used for the SSRF.

Table 2 .The monitors for SSRF beam diagnostic

monitor	Linac	L T B	Booster	B T S	Storage Ring	Total
BPM	3	3	54	3	150	213
DCCT			1		1	2
Wall Current	1		1		1	3
Stripline			2		2	4
Profile	3	5	4	6	7	25
Beam Loss	10		Some	8	86	110
Slit		2		2		4
Beam Current	3	5		6		11
SRM			1		1	2
Scraper					2	2
Global Feedback					1	1
Faraday Cup	1					1

2 BEAM POSITION

2.1 Beam position monitor

One of the basic functions of any accelerator beam instrumentation and control systems, the BPM data are used to correct the closed orbit distortion (COD) and to perform the local beam steering for the synchrotron radiation beam lines. Measurements of the dispersion functions are also implemented by the reliable beam position measurements. The button-type electrodes, which are capacitive, coupled to the beam, are now most popular with the electron storage rings because they occupy very little longitudinal space and have a simple structure with low cost and small coupling impedance. The beam position is measured by four-button electrodes, which mounted on the SMA-type feedthroughs.

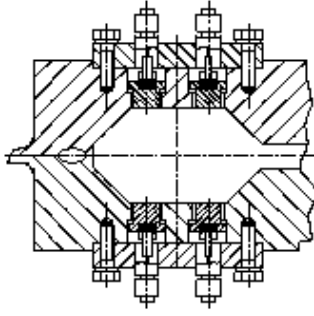


Fig.1 the schematic cross section of the beam position monitor

The feedthrough is similar Ceramaseal Company type 11605-04-w SMA connector in SSRF storage ring. The diameter of the button is selected as 15 mm to reduce the pickup beam power at the large beam intensity. Fig.1 shows the schematic cross section of the beam position monitor. In order to improve the measurement precision, the mechanical deformation and the assembly error for each BPM unit must be minimized

2.2 Theoretical analysis

We have done theoretical analysis with Green-function method. The electrostatic field is given by a Laplace equation; we solved it numerically by the boundary element method. When the boundary element is small enough, the charge density $\sigma_l(s)$ is approximated to be constant within the element. The boundary element method gives accurate solutions using only a small number of boundary elements. The potential of kth element can be represents by two terms as following equation:

$$\phi_k = \frac{1}{2\pi\epsilon_0} \left(\ln \frac{1}{r_{0k}} + \sum_{l=0}^N \sigma_l \int_s \ln \frac{1}{r_{kl}} ds \right)$$

The first term is the potential produced by the beam charge, r_{0k} is the distance from beam to the center of kth element and the second one by induced charge of all boundary elements, r_{lk} is the distance from lth to kth element.

Because of the nonlinear response of such monitors, the experimental data need to be corrected by using a nonlinear limited square fitting in order to reconstruct the beam position. In the great majority of cases, ours included, a polynomial fitting function is used.

There are N elements on the boundary, so that gives the following matrix equation. It is a useful tool to calculate the position sensitivity of a position monitor. The software “MathCAD” used to do this work.

$$\frac{1}{2\pi\epsilon_0} \cdot [\phi_k] = [G_{0k}] + [G_{kl}] \cdot [\sigma_l]$$

G is the Green’s function. Vacuum chamber is connected to the ground, so the potential of the boundary

$$[G_{0k}] + [G_{kl}] \cdot [\sigma_l] = 0$$

is zero.

The induced charge distribution σ_l is obtained from following equation.

$$[\sigma_l] = -[G_{kl}]^{-1} \cdot [G_{0k}]$$

The normalized electrical position (H, V) can get from induced charge. X and Y obtained from equation.

$$X = \sum_{i=0}^4 \sum_{j=0}^i A_{i-j,j} H^{i-j} V^j \quad Y = \sum_{i=0}^4 \sum_{j=0}^i B_{i-j,j} H^{i-j} V^j$$

For the BPM geometries with four electrodes, a convenient arrangement, show in Fig. 2.

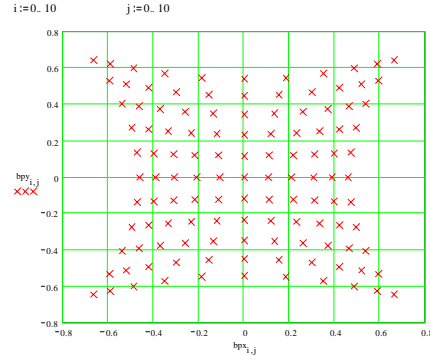


Fig2. Position map of caculation for cylindrical BPM

Where A_{i-j} , B_{i-j} , are polynomial function while $A_{0,0}$ and $B_{0,0}$ are the BPM offsets. When the mechanical tolerances of the BPM are small not all of the polynomial terms are used. When bound is divided 110 elements, 10th order fitting, the fitting error is less than 10^{-7} m in 10mm *10mm area.

We designed storage ring BPM monitor by this method. While the distance between x direction two buttons equal to 25mm, the sensitivity (S) in mm^{-1} of X and Y are similar in our case. $1/S_x=17.0$; $1/S_y=16.6$. While disdance equal to 25.6mm $1/S_x=16.7$; $1/S_y=16.7$.

The calibration values are in good agreement with the experiment values by test set using a calibration wire.

2.3 Calibration of BPM

Bench calibration to a prototype BPM is carried out in the laboratory with a wire movable to find out the offset valume and BPM sensitivity. Beam base alignment method will be used in future.

There is a detail description about this equipment in these proceedings. We know the wire setting error from mechanical measurements using raster ruler. The resolution has been reached to 1 μ m. From the original position the wire is moved step-by-step over the desired area in the center of BPM assembly. The step length of motor is 2 μ m .At 500MHz, the coupling impedance of the buttons to wire is low, so high sensitivity Bergozelectronics are used to measure. This work also can done by pre-amplifier to boost the signals and measured by HP4396B spectrum analyzer. RF switch is

used to select signals. The measurement is completely automatic. Labview provide easy to use interface and environment. The measurement can do from internet; it's very useful for anti-induction at 500MHz high frequency.

For this system, mechanical adjusting error is less than $10\ \mu\text{m}$; as well as the resolution is $2\ \mu\text{m}$. Curve-fitting in MathCAD was used to extract polynomial coefficients from the experimental data using the least square method. The system electronics stability in 8 hours is less than 3mV; the fitting error in X is about $6 \cdot 10^{-3}\text{mm}$ and Y is about $8 \cdot 10^{-3}\text{mm}$. It's good enough for the calibration.

3 SYNCHROTRON LIGHT MONITOR

Because the wavelength λ is long compared with the critical wavelength, the diffraction limit scales as $\lambda^{2/3}$. The SSRF SLM will use wavelength of 210nm (near ultraviolet).The parameter of SSRF synchrotron light monitor is shown in table.4.

Table.4 The Parameter of SSRF synchrotron monitor

Parameter	Parameter
Radius of curvature in dipole ρ	10.568m
Critical energy in dipole E_c	8.993Kev
Critical wavelength in dipole λ_c	0.137nm
Measurement wavelength	210nm \pm 5%
Opening angle ($1/\nu$) at λ_c	0.17mrad
Diffraction spot size σ_d	16.2 μm
Electron beam size σ_x	147 μm
Electron beam size σ_y	50 μm

The synchrotron light emitted in a bending magnet of the storage ring is a very important beam diagnostic source since the length and transverse size of the light pulse are almost the same as those of the electron beam. The synchrotron light is reflected through the window by a water-cooled mirror in the vacuum chamber and then directed by a remote controlled mirror to an optical bench supporting the diagnostic instruments in a dark room. A CCD camera provides the beam profile on a TV monitor in the control room. The beam height and width are measured with a lens system focusing the synchrotron light on a two-dimensional solid state scanned photodiode array, such as the EG&G Reticons. The bunch length for a single pass is measured with a streak camera with 2 ps resolution, such as Model C5680-11 of Hamamatsu. The averaged bunch length over many turns can be measured with a fast micro-channel tube and sampling oscilloscope system or with a real time bunch length monitoring system using beam spectrum.

A visible light data acquirment and analysis has been established with a CCD camera and photodiode array of the EG&G Reticons. For Camera, minimum illumination 0.01 lux; S/N ratio More than 46dB; data acquiring speed 30MHz. The advanced 2D and 3D visualization tools of Labview as Fig.3, let us insight into data and immediately visualize the data. The beam size FWHM of X and Y are shown on the screen lively. It can be shown via internet. Linear array resolution is $25\ \mu\text{m}$.

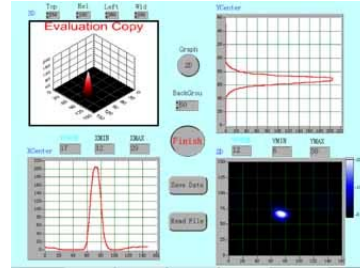


Fig3. The display of 2D and 3D for visible light on the screen

4 CONCLUSION

This paper is not intended to be a comprehensive review of light source beam diagnostics; we have chosen to report on SSRF diagnostic system that will be used to measure basic accelerator parameters. Our focus is on measurement and commissioning of close orbit in the storage ring. Only BPM and SLM monitor, BPM calibration equipment design for prototype testing is described.

5 ACKNOWLEDGMENTS

The authors would like to thank S.Smith J.Hinkson Kaiichi Haga for their comments and helps. Also thanks S. Y. Chen Z. T. Zhao and D. K. Liu encouragement and correction.

REFERENCES

- [1] Ye Kairong Liu Dekong Zhou Weiming Chen Yonzon "Beam Instrumentation for SSRF" *The 9th Beam instrumentation Workshop (BIW'00)*, May 2000 published by "The American Institute of Physics"
- [2] Alan S.Fisher. , Instrumentation and Diagnostics for PEP-II, *SLAC-PUB-7835*, May 1998
- [3] Barrett. I., et al., "Dynamic Beam Based Calibration of Orbit Monitors at LEP," *Proceedings of the 4th International Workshop on Accelerator Alignment*, Tsukuba, Japan, December 1995, KEK Proc. 95-12 and CERN-SL/95-97 (BI).
- [4] Corbett, W.J., R.O. Hettel, and H.D. Nuhn. "Quadrupole Shunt Experiments at SPEAR" (SLAC-PUB-7162), presented at the 7th Beam Instrumentation Workshop (BIW 96), Argonne, IL, May 1996.